Influence of Cation (RE = Sc, Y, Gd) and O/H Anion Ratio on the Photochromic Properties of REO_xH_{3-2x} Thin Films

Giorgio Colombi,* Tom De Krom, Diana Chaykina, Steffen Cornelius, Stephan W. H. Eijt, and Bernard Dam

ACCESS | Metrics & More | Article Recommendations | Supporting Information

ABSTRACT: Rare-earth oxyhydride REO_xH_{3-2x} thin films prepared by air-oxidation of reactively sputtered REH_2 dihydrides show a color-neutral, reversible photochromic effect at ambient conditions. The present work shows that the O/H anion ratio, as well as the choice of the cation, allow to largely tune the extent of the optical change and its speed. The bleaching time, in particular, can be reduced by an order of magnitude by increasing the O/H ratio, indirectly defined by the deposition pressure of the parent REH_2. The influence of the cation (RE = Sc, Y, Gd) under comparable deposition conditions is discussed. Our data suggest that REs of a larger ionic radius form oxyhydrides with a larger optical contrast and faster bleaching speed, hinting to a dependency of the photochromic mechanism on the anion site-hopping.

KEYWORDS: oxyhydrides, photochromic, anions, oxide, hydride, positron annihilation, lanthanides, diffusion
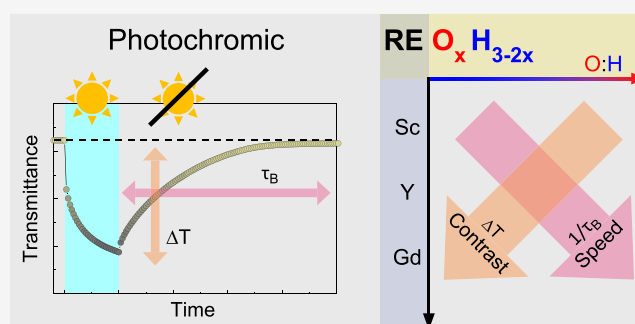
While the properties of single-anion compounds, like the metal oxides, are to a large extent dictated by their cation chemistry, multianion compounds offer unprecedented degrees of freedom in the design of functional materials thanks to the broad spectrum of different anion characteristics, such as electronegativity, polarizability, and ionic radii.[1,2] Within this class of materials, rare earth (RE) oxyhydride REO_xH_{3-2x} compounds stand out not only for their exceptional H^- conductivity,[3,4] but also for the possibility of preparing them via post-oxidation of reactively sputtered REH_2 thin films: a route of synthesis that allows indirect control over the resulting microstructure and O/H ratio.[5]

Since the first report in 2011,[6] REO_xH_{3-2x} oxyhydride films prepared in this way (with RE = Sc, Y, Gd, Dy, and Er and $0.5 \leq x < 1.5$) have gathered increasing attention in view of their color-neutral reversible photochromic effect and photoconductivity at ambient conditions, making them promising candidates for smart windows and sensors.[5,7,8]

While such optical behavior is shared by many REs, it remains unexplored what is the root of such generality and the influence of the cation. In addition, the physical mechanism behind the photochromic effect is unclear, as well as its limits in terms of optical contrast and speed.

The present work exemplifies the tunability of the RE multianion compounds and contributes to the understanding of these materials by surveying the effect of both the cation and the O/H anion ratio on the photochromic contrast and speed of RE oxyhydride thin films.

First, we show that the deposition pressure of the parent (i.e., as-grown) REH_2 indirectly defines the anion ratio of the final oxyhydride, as well as its porosity and lattice constant. Consequently, optical properties such as the refractive index, optical band gap, and photochromic behavior can be tuned. We report that the bleaching time constant, in particular, can be reduced by an order of magnitude to below 10 min by an optimal choice of the deposition pressure.

Second, by having mapped the effect of the deposition pressure on the photochromic properties of Sc, Y, and Gd oxyhydrides, we address the influence of the cation under comparable deposition conditions. Our data suggest that REs of higher atomic number and larger ionic radius form oxyhydrides with better photochromic properties, that is, larger optical contrast and faster bleaching speed.

Sc-, Y-, and Gd-based REH_2 thin films (thickness ∼ 150 nm) were prepared by reactive magnetron sputtering of a 2 in. metal target (MaTeck Germany, 99.9% purity) in a Ar/H_2 (5N purity) atmosphere. The deposition chamber was kept at a base pressure below 1×10^{-6} Pa. During deposition the total gas flow was fixed at 40 sccm with an Ar/H_2 gas ratio of 7:1,
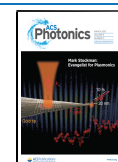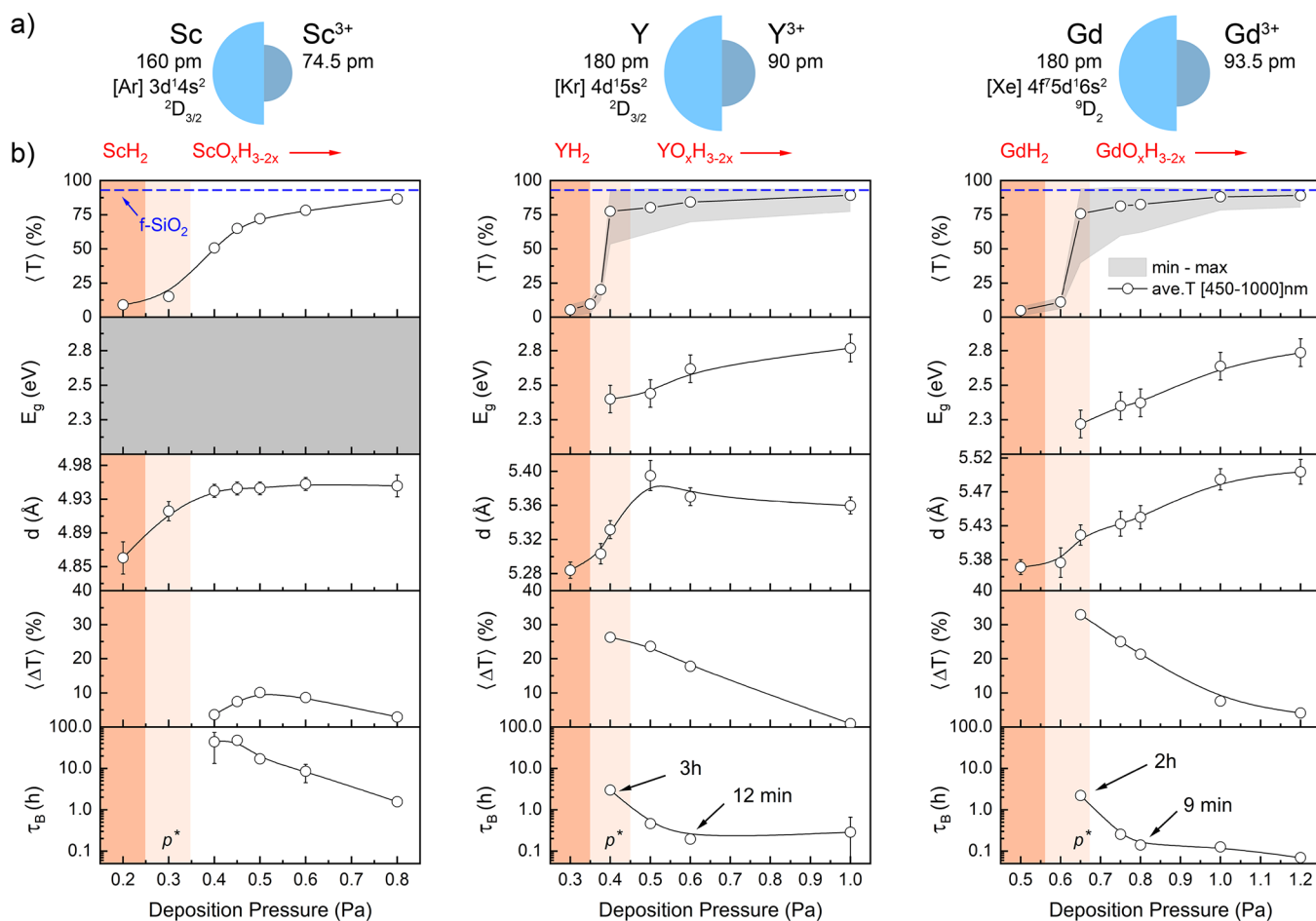
Figure 1. (a) Radius,[9] ground state electron configuration, and term symbols for Sc, Y, and Gd atoms. The Shannon effective radii of their trivalent ions are also given.[10] (b) Effect of deposition pressure of the parent REH_2 dihydride (RE = Sc, Y, Gd) on the key material properties of the resulting REO_xH_{3-2x} after exposure to air. From top to bottom: min, max, and average optical transmittance ($\langle T \rangle$), optical band gap (E_g), lattice constant (d), photochromic contrast ($\langle \Delta T \rangle$), and photochromic bleaching time (τ_B). A higher deposition pressure results in a higher porosity and, consequently, higher oxygen content. Samples sputtered at pressures below the critical pressure p^* (dark orange background) do not incorporate oxygen upon air exposure and remain optically thick REH_2 metal hydrides. Around p^* (light orange background) the metal to semiconducting REO_xH_{3-2x} transition sets in. Films sputtered at $p \sim p^*$ show composition gradients, with higher oxygen concentration at the film surface (Figure S3). Only at higher deposition pressures ($p > p^*$), single-phase homogeneous photochromic oxyhydrides are obtained. A further increase in deposition pressure leads to an increasing O/H ratio (Figure S3), decreasing photochromic contrast, and faster bleaching.

while the total deposition pressure (p_{dep}) was varied by means of a butterfly reducing valve mounted at the inlet of the pumping stage. The DC power supplied to the Sc, Y, and Gd targets was set at 200, 200, and 165 W, respectively, corresponding to metal deposition rates of 1.2, 3.0, and 3.0 Å/s. All samples were grown on unheated UV-grade fused silica (f-SiO₂) and polished glassy carbon substrates.

The as-deposited REH_2 thin films were then oxidized in ambient conditions by exposure to air. Since the oxidation is a self-limiting process, after a few days in air the samples reach a (meta)stable state (Figure S1). All material characterization presented in this work was done only after such a stable condition was reached. Structural and optical properties were studied by a combination of X-ray diffraction (XRD, Bruker D8 Discovery) and photospectrometry. A custom-built optical-fiber based *in-situ* spectrometer (range: 230−1150 nm) with a time resolution of ∼1 s was employed to test the photochromic effect as triggered by a narrow-band LED (λ = 385 nm, I = 75 mW/cm²). Throughout this work, all values of average transmittance, $\langle T \rangle$, refer to the interval λ: [450, 1000] nm. The REO_xH_y chemical composition was studied by a

combination of Rutherford backscattering spectrometry (RBS) and elastic recoil detection (ERD) at the 2 MV Van-de-Graaff accelerator at Helmholtz-Zentrum Dresden-Rossendorf (Dresden, Germany).[5] A series of thicker (∼450 nm), Al-capped (∼20 nm) Y oxyhydrides produced in the same way were studied by Doppler Broadening positron annihilation spectroscopy (DB-PAS) at the Variable Energy Positron (VEP) facility located at the Reactor Institute Delft (Netherlands). The aforementioned 385 nm LED was used for *in-situ* illumination (2.5 h), although with a reduced irradiance (I = 30 mW/cm²) due to the larger distance between the light source and the sample.
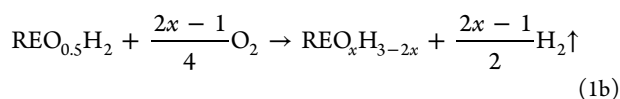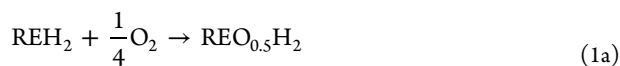
Figure 1 shows the impact of the deposition pressure of the parent REH_2 dihydride on the key material properties of the resulting REO_xH_{3-2x} after exposure to air. We observe similar trends in Sc, Y, and Gd oxyhydrides, whose cations, respectively, belong to the fourth, fifth, and sixth periods of the periodic table and, albeit maintaining a similar chemistry and valence electron configuration, represent a wide range of ionic radii within the group of REs (Figure 1a). Sc is the smallest extreme, while Gd is a good proxy for the largest

lanthanides. Therefore, we suppose that these trends are general to virtually any RE that forms stable oxyhydrides.

In Figure 1b we distinguish three regions, reflecting the onset of the oxidation and the metal REH_2 dihydride to semiconducting $REO_xH_{3−2x}$ oxyhydride transition. Nafezarefi et al.[7] reported that oxygen incorporates only in RE dihydride thin films sputtered at a sufficiently high deposition pressure, above a threshold value (critical pressure, $p*$) that depends on the RE and on the specificities of the sputtering chamber. Above this pressure, the metal-to-insulator transition takes place when exposing the thin film to air: an optical bandgap opens and the transmittance maxima at $E < E_g$ approach the value of the bare substrate, implying the absence of a second absorbing/scattering phase and a negligible concentration of deep, optically active defects.[7] We recognize this behavior in Y and Gd oxyhydrides (Figure 1b, top panel), while the absorption spectra of Sc-based compounds show a prominent absorption tail (Figure S2) that extends to the whole measured spectral range and impedes the evaluation of the optical bandgap from the transmittance spectra.

RBS/ERD data show that the Sc, Y, and Gd oxyhydride thin films sputtered at pressures near $p*$ (0.3, 0.375, and 0.6 Pa, respectively) present a composition gradient throughout their thickness, resembling the diffusion profile of oxygen starting from the film surface. Only at higher deposition pressures homogeneous photochromic oxyhydrides are obtained (Figure S3). RBS/ERD data additionally verify that a higher deposition pressure results in a higher O/H ratio, in qualitative agreement with the progressive decrease of the refractive index, as implied by the decreasing amplitude of the thin-film interference oscillations (Figures S2 and 1b, top panel), and with previous studies on both Y and Gd oxyhydride thin films.[8,11,12]

We argued recently that the reaction from metallic REH_2 dihydride to photochromic $REO_xH_{3−2x}$ oxyhydride happens in two steps:[5,13] first, a net oxygen incorporation (eq 1a); second, a continuous oxygen-for-hydrogen (1:2) exchange (eq 1b).[13]

$$REH_2 + \frac{1}{4}O_2 \rightarrow REO_{0.5}H_2 \tag{1a}$$

$$REO_{0.5}H_2 + \frac{2x-1}{4}O_2 \rightarrow REO_xH_{3−2x} + \frac{2x-1}{2}H_2\uparrow \tag{1b}$$

These reactions are driven by a large gain in lattice energy and occur spontaneously even at ambient conditions when the kinetic barriers of oxygen diffusion are not prohibitive.[13] In this context, porosity is an enabling factor for the formation of RE-oxyhydrides via post oxidation of sputtered REH_2 thin films. As depicted in the well-known sputtering zone diagram,[14] a higher deposition pressure translates to a higher porosity because of the increased probability of collisions of the sputtered atoms in the gas phase and, therefore, a reduced kinetic energy once they reach the substrate. Thus, higher deposition pressures lead to higher O/H ratios due to the increased porosity of the films.

Though we can tune the O/H ratio by the deposition pressure, we find that this is limited to the H-rich range ($0.5 < x < 1$) of the $REO_xH_{3−2x}$ composition line. Indeed, the optical band gap gradually increases from 2.3(1) eV to 2.8(1) eV (Figure 1b, second panel) and, by comparison to the phenomenological relation that links E_g and composition,[5] shows that all the oxyhydrides investigated here belong to the H-rich region. Hence, in agreement with our previous ion-

beam analysis,[5] it appears that O-rich oxyhydrides ($x > 1$) with $E_g \geq 3$ eV do not form via air exposure of highly porous REH_2 films at room temperature. This might relate to the limited driving force for further oxygen inclusion at $x > 1$,[13] as well as to the substrate-induced strain that hinders the further lattice expansion and distortion that is expected for compositions that approach the bixbyite oxide.

While no obvious structural phase change is observed from the fcc-$Fm\overline{3}m$ structure motif of the parent dihydride (Figure S4), we notice, in agreement with previous works,[5,7] that the oxidation to the oxyhydride state is accompanied by a lattice expansion (Figure 1b, third panel). Our data show that reaction 1a, which coincides with the oxidation of the cation from RE^{2+} to RE^{3+} and with the metal to semiconductor transition, is always accompanied by a lattice expansion, intuitively needed to accommodate the additional $O^{2−}$ anions. The volume changes corresponding to reaction 1b appear instead to be different from cation to cation, with Sc plateauing, Y showing a weak maximum, and Gd expanding monotonously for increasing deposition pressures.

The lower two panels in Figure 1b show the dependence of the photochromic properties of Sc, Y, and Gd oxyhydrides on the deposition pressure. While the full cycles of photo-darkening (30 min) and bleaching are reported in Figure S5, we introduce here two figures of merit to quantitatively express the photochromic behavior in terms of the application-limiting aspects, namely, the magnitude of the optical change and its speed. First, we define the absolute contrast, $\langle \Delta T \rangle$, as the difference between the initial average transmittance, $\langle T_0 \rangle$, and that at the end of the darkening, $\langle T_{dark} \rangle$:

$$\langle \Delta T \rangle = \langle T_0 \rangle - \langle T_{dark} \rangle \tag{2}$$

Second, we address the bleaching speed via a characteristic time constant, τ_B, which reflects the time required for the material to revert to its initial transmittance after the illumination is ceased. Under the only hypothesis that all absorbing species formed during illumination disappear following reaction kinetics of equal order, τ_B is equal to the inverse of the weighted-average rate at which the photo-generated absorbing species disappear. Assuming a first order bleaching kinetics, eq 3 is employed in Figure S5 to derive the bleaching time constant from the time evolution of the average optical transmittance $\langle T(t) \rangle$:[15]

$$\ln\left(-\ln\frac{\langle T(t) \rangle}{\langle T_0 \rangle}\right) = -\frac{1}{\tau_B}t - \ln\langle T_{dark} \rangle \tag{3}$$

A higher deposition pressure leads to photochromic Sc, Y, and Gd oxyhydrides of lower absolute contrast and significantly shorter bleaching time. The latter, in particular, is reduced by an order of magnitude, from tens of hours to some hours for Sc-based oxyhydrides and from few hours to few minutes for Y- and Gd-based oxyhydrides. It appears that the atomic number of the cation and, even more, its size correlate with overall better photochromic properties, that is, larger contrast and faster kinetics. The ~150 nm Gd oxyhydride films produced at higher pressures, with a bleaching time constant below 10 min, present the best bleaching kinetics among the RE oxyhydrides thin films studied here. At the time of writing, quantitative analysis of the bleaching kinetics can be found only in refs 8 and 13, where time constants on the order of several hours are reported for

bare and Zr-doped Y oxyhydride films. Similarly long bleaching times can be qualitatively observed also elsewhere.[7,16]

While the relations between deposition pressure (i.e., composition), optical band gap, and lattice constant are fairly well understood, the mechanism behind the photochromic effect remains unclear. The bandgap excitation points to an electronic origin; yet, at present, it is not known if other electronic processes follow the interband absorption. In any case, the large time constants involved in the photochromism suggest that structural rearrangement might play a dominant role. In this sense, it was hinted that the photodarkening depends on the segregation of an absorbing phase,[17,18] a process accompanied by reversible contraction of the crystal lattice[16,19] and quenching of the NMR signal of the most mobile H fraction ($\sim$3%).[20] Hence, in the following we consider the influence of the deposition pressure on both electronic and structural properties and support our discussion with the insight from DB-PAS on Y-based thin films.

In Figure 2, reference materials and photochromic oxyhydrides sputtered at different deposition pressures are
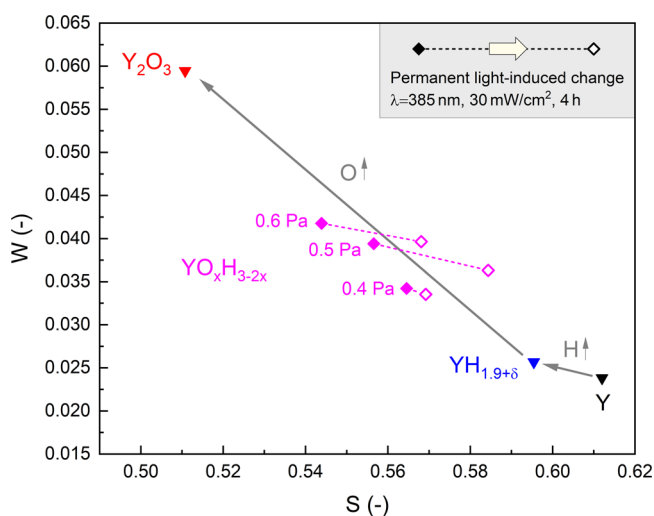

Figure 2. DB-PAS S/W diagram of the Y to YH$_2$ to Y$_2$O$_3$ composition range, including YO$_x$H$_{3-2x}$ oxyhydrides sputtered at different deposition pressures in their virgin state (full points). The arrows indicate the general trends in S/W for the transition from metallic Y to metallic YH$_2$ (hydrogenation) to insulating Y$_2$O$_3$ (oxidation). The open points show the permanent light-induced change in the S/W of the oxyhydrides after a full cycle of photodarkening (4 h) and bleaching in the dark (72 h).

mapped versus the so-called line shape DB-PAS parameters W and S, which indicate the probability of positron annihilation with electrons of high momentum (e.g., (semi)-core states) and low momentum (e.g., semiconductor valence states), respectively. We have already mentioned that the deposition pressure influences the final composition and, hence, the optical bandgap. Accordingly, DB-PAS shows a trend of increasing W and reduced S parameters upon an increased O/H ratio, indicating a broadening of the electron momentum distribution as the valence band gains a progressively larger O(2p) character. This supports the hypothesis, originally advanced by Cornelius et al.[5] in analogy to other multi anion compounds, that the valence band of RE oxyhydrides is a mixture of occupied H(1s) and O(2p) states, and that it shifts toward lower energies with increasing O/H

ratio because of the higher electronegativity of oxygen (χ_O = 3.44) compared to hydrogen (χ_H = 2.20).

After a full cycle of photodarkening and bleaching, we observe irreversible changes in the S/W parameters of all samples, evidence that permanent light-induced structural modifications occur in Y oxyhydrides sputtered at any deposition pressure. In particular, we find the same trend originally reported by Plokker et al.,[21] where upon *in-situ* illumination S increases and W decreases, suggesting a permanent formation of positron trapping sites that might include negatively charged cation monovacancies (V_Y) or neutrally charged vacancy clusters (e.g., $V_Y - V_H$, $V_H - V_H$, $V_O - V_H$).[21,22] Visually, we note that the direction of the change in the S/W plot is similar for all samples. This is quantified by the so-called R parameter ($R = \Delta S / \Delta W$), a defect-specific value that is independent of the concentration of defects and on the positron trapping efficiency.[23] For YO$_x$H$_{3-2x}$ sputtered at 0.4, 0.5, and 0.6 Pa we find, respectively, $R = -7(5)$, $R = -9(1)$, and $R = -11(3)$. While further studies are needed to exactly identify the vacancies that irreversibly form upon photo-darkening, the fact that all samples show a similar R parameter suggests that the deposition pressure does not influence the type of formed negative and neutral vacancies seen by DB-PAS. This vacancy formation under modest illumination conditions indicates the local mobility/displacement of ions in the RE oxyhydrides induced by photoexcitation. However, we exclude that the involvement of these vacancies is a necessary condition for the bleaching to occur, since no reversibility over time is observed in the oxyhydrides deposited at 0.5 and 0.6 Pa (Figures S6 and S7).

Let us now look at the implications of a change in O/H ratio in more detail. Recently we verified that for any oxyhydride composition (REO$_x$H$_{3-2x}$ with $0.5 \leq x \leq 1.5$) the O^{2-} anions are located in the tetrahedral interstitial sites defined by the cation lattice.[13] On that basis, we proposed an idealized structure model that serves as a guideline to estimate the fraction and type of free interstitial sites, depending on the anion ratio. Figure 3 shows the correlation between this structural model and the trend observed in this work of decreasing photochromic contrast and increasing bleaching speed upon O/H ratio.

We suppose that RE oxyhydride thin films share the exceptional H$^-$ conductivity of the bulk RE oxyhydrides,[3,4] and that the mobility of the hydride ions is an enabling factor for the photodarkening. While there is yet no data available for either local or long-range hydrogen motion in REO$_x$H$_{3-2x}$ thin films, LaO$_x$H$_{3-2x}$ powders show higher H$^-$ ionic conduction at lower O/H anion ratio (i.e., lower x).[3] Comparing to the trend of photochromic contrast in the compositional interval $0.5 < x < 1$, the bulk diffusion of H$^-$ ions might then influence the overall extent of the photochromic process: the increase in contrast would then be related to an increase in the H$^-$ diffusion coefficients. In this range of compositions, we suggest that H$^-$ ions move either via direct hopping between neighboring octahedral sites or via the indirect hopping mediated by tetrahedral vacancies, in analogy to what is proposed for other fluorite-type anion conductors, such as LnOH (with Ln = La, Nd),[4] β-PbF$_2$,[24] and β-PbSnF$_4$.[25] Conversely, we expect direct tetrahedral-based mobility to be severely inhibited by the lack of free tetrahedral sites and by the high activation energy.[4] In this sense, we point out that the Y and Gd oxyhydrides produced, respectively, at 1.0 and 1.2 Pa are only weakly photochromic ($\langle \Delta T \rangle$ < 4%) and their E_g =
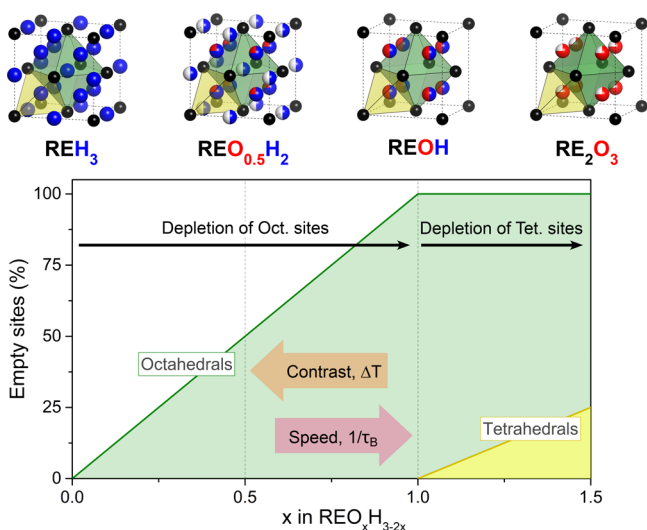
Figure 3. Fraction of empty octahedral (green polygons) and tetrahedral (yellow polygons) interstitial sites upon increasing the O/H ratio in fcc, anion-disordered REO_xH_{3-2x} oxyhydrides. The arrows indicate the correlation with the photochromic contrast and bleaching time constant.

2.8(1) eV suggests a composition that approaches the stoichiometric REOH.[5] Possibly the photochromic properties of oxyhydrides of a composition close to $x = 1$ are suppressed due to their specific interstitial-site occupation (tetrahedrals all occupied and octahedrals all empty), which hinders the aforementioned diffusion pathways and therefore reduces the attempt frequency for site hopping and the anion mobility altogether.[3] Finally, it cannot be excluded that also the diffusion of oxygen plays a role, as suggested by Baba et al.[16] When compared to the rate of hydrogen hopping, however, the oxide sublattice of bulk oxyhydrides is found essentially stationary by computational[3,4,26−28] and experimental[29,30] works alike. Intuitively, the reason lies in the lower polarizability and double charge of the O^{2-} oxide ions compared to H^- hydride ions.[1]

The fact that we could rationalize (i) composition, (ii) optical transmittance, (iii) optical bandgap, (iv) lattice constant, and (v) trends in photochromic properties within the framework of a single-phase line-compound strongly indicates that the photochromism is an intrinsic property of the REO_xH_{3-2x} oxyhydride phase. We note that the alternative hypothesis of Hans et al.,[31] who recently proposed the coexistence of an oxide and a dihydride phase, is not compatible with the well-established optical bandgaps and complete transmittance for $E < E_g$ of REO_xH_{3-2x} thin films. Conversely, our careful study of the oxidation behavior and its dependency on the deposition pressure can explain the specific composition reported by Hans et al. as that of a partially oxidized REH$_2$, a nongeneral case that we obtain only around p^*. However, we do not exclude the possibility of domains with slightly reduced/increased oxygen or hydrogen content, that is, small local variations of x within the REO_xH_{3-2x} phase. In analogy to what is observed in mixed halide perovskites, as recently reviewed by Brennan et al.,[32] local compositional inhomogeneity of this type might facilitate structural rearrangements upon illumination.

In summary, we have systematically shown that the photochromic properties of REO_xH_{3-2x} oxyhydrides thin films, namely, the photochromic contrast and the bleaching

kinetics, can be largely tuned by controlling the deposition pressure of the parent REH$_2$. We suppose that the root of this tunability lies in the different O/H anion ratio and, consequently, in the different number and energetics of the empty sites that enable anion hopping and therefore facilitate the structural rearrangements thought to occur during the photochromic process. DB-PAS shows vacancy formation during photodarkening, indicating local mobility of ions as a consequence of photoexcitation of charge carriers. However, the observed vacancy formation is irreversible and does not play an essential role in the bleaching process. The photochromic properties of oxyhydrides of different REs are compared in a comprehensive way, showing a trend of increasing contrast and bleaching speed from Sc- to Y- to Gd-based oxyhydrides. While a conclusive answer on the role of the cation is still missing, we note that these trends and their correlation to the cation size hint once again to a process limited by diffusion. As a matter of fact, the cation size translates to a larger lattice constant, 4.94(4) Å for Sc, 5.36(4) Å for Y, and 5.45(6) Å for Gd oxyhydrides, reducing the activation barriers for site hopping.[4] However, we do not exclude that other factors indirectly influenced by the deposition pressure might play a role in the photochromic process, for example, porosity, grain size, defects, texture, stress, and degree of anion ordering.

The fact that we could produce photochromic films that bleach in less than 10 min brings the RE oxyhydrides one step closer to applications as smart coatings for sensors and windows.

■ ASSOCIATED CONTENT

ⓢ Supporting Information

The Supporting Information is available free of charge at https://pubs.acs.org/doi/10.1021/acsphotonics.0c01877.

> Transmittance spectra and Tauc plots, RBS/ERD spectra, XRD patterns, time-resolved measurements of (i) optical transmittance and (ii) DB-PAS during darkening and bleaching, and additional details on DB-PAS analysis (PDF)

■ AUTHOR INFORMATION

Corresponding Author

Giorgio Colombi — *Materials for Energy Conversion and Storage, Department of Chemical Engineering, Delft University of Technology, NL-2629HZ Delft, The Netherlands;* ● orcid.org/0000-0001-6424-7684; Email: g.colombi@tudelft.nl

Authors

Tom De Krom — *Fundamental Aspects of Materials and Energy, Department of Radiation Science and Technology, Faculty of Applied Sciences, Delft University of Technology, NL-2629 JB Delft, The Netherlands;* ● orcid.org/0000-0003-4269-4330

Diana Chaykina — *Materials for Energy Conversion and Storage, Department of Chemical Engineering, Delft University of Technology, NL-2629HZ Delft, The Netherlands; Fundamental Aspects of Materials and Energy, Department of Radiation Science and Technology, Faculty of Applied Sciences, Delft University of Technology, NL-2629 JB Delft, The Netherlands;* ● orcid.org/0000-0002-2872-6415

Steffen Cornelius − *Materials for Energy Conversion and Storage, Department of Chemical Engineering, Delft University of Technology, NL-2629HZ Delft, The Netherlands; Fraunhofer Institute for Organic Electronics, Electron Beam and Plasma Technology (FEP), 01277 Dresden, Germany;* ◉ orcid.org/0000-0002-0358-7287

Stephan W. H. Eijt − *Fundamental Aspects of Materials and Energy, Department of Radiation Science and Technology, Faculty of Applied Sciences, Delft University of Technology, NL-2629 JB Delft, The Netherlands;* ◉ orcid.org/0000-0002-7399-6043

Bernard Dam − *Materials for Energy Conversion and Storage, Department of Chemical Engineering, Delft University of Technology, NL-2629HZ Delft, The Netherlands;* ◉ orcid.org/0000-0002-8584-7336

Complete contact information is available at:
https://pubs.acs.org/10.1021/acsphotonics.0c01877

Notes
The authors declare no competing financial interest.

REFERENCES

(1) Kageyama, H.; Hayashi, K.; Maeda, K.; Attfield, J. P.; Hiroi, Z.; Rondinelli, J. M.; Poeppelmeier, K. R. Expanding frontiers in materials chemistry and physics with multiple anions. *Nat. Commun.* **2018**, *9*, 772.

(2) Kobayashi, Y.; Hernandez, O.; Tassel, C.; Kageyama, H. New chemistry of transition metal oxyhydrides. *Sci. Technol. Adv. Mater.* **2017**, *18*, 905−918.

(3) Fukui, K.; Iimura, S.; Tada, T.; Fujitsu, S.; Sasase, M.; Tamatsukuri, H.; Honda, T.; Ikeda, K.; Otomo, T.; Hosono, H. Characteristic fast H⁻ ion conduction in oxygen-substituted lanthanum hydride. *Nat. Commun.* **2019**, *10*, 2578.

(4) Ubukata, H.; Broux, T.; Takeiri, F.; Shitara, K.; Yamashita, H.; Kuwabara, A.; Kobayashi, G.; Kageyama, H. Hydride Conductivity in an Anion-Ordered Fluorite Structure LnHO with an Enlarged Bottleneck. *Chem. Mater.* **2019**, *31*, 7360−7366.

(5) Cornelius, S.; Colombi, G.; Nafezarefi, F.; Schreuders, H.; Heller, R.; Munnik, F.; Dam, B. Oxyhydride Nature of Rare-Earth-Based Photochromic Thin Films. *J. Phys. Chem. Lett.* **2019**, *10*, 1342−1348.

(6) Mongstad, T.; Platzer-Björkman, C.; Maehlen, J. P.; Mooij, L. P.; Pivak, Y.; Dam, B.; Marstein, E. S.; Hauback, B. C.; Karazhanov, S. Z. A new thin film photochromic material: Oxygen-containing yttrium hydride. *Sol. Energy Mater. Sol. Cells* **2011**, *95*, 3596−3599.

(7) Nafezarefi, F.; Schreuders, H.; Dam, B.; Cornelius, S. Photochromism of rare-earth metal-oxy-hydrides. *Appl. Phys. Lett.* **2017**, *111*, 103903.

(8) You, C. C.; Mongstad, T.; Marstein, E. S.; Karazhanov, S. Z. The dependence of structural, electrical and optical properties on the composition of photochromic yttrium oxyhydride thin films. *Materialia* **2019**, *6*, 100307.

(9) Slater, J. C. Atomic Radii in Crystals. *J. Chem. Phys.* **1964**, *41*, 3199−3204.

(10) Shannon, R. D. Revised effective ionic radii and systematic studies of interatomic distances in halides and chalcogenides. *Acta Crystallogr., Sect. A: Cryst. Phys., Diffr., Theor. Gen. Crystallogr.* **1976**, *32*, 751−767.

(11) You, C. C.; Mongstad, T.; Maehlen, J. P.; Karazhanov, S. Engineering of the band gap and optical properties of thin films of yttrium hydride. *Appl. Phys. Lett.* **2014**, *105*, 031910.

(12) Baba, E. M.; Montero, J.; Moldarev, D.; Moro, M. V.; Wolff, M.; Primetzhofer, D.; Sartori, S.; Zayim, E.; Karazhanov, S. Preferential Orientation of Photochromic Gadolinium Oxyhydride Films. *Molecules* **2020**, *25*, 3181.

(13) Colombi, G.; Cornelius, S.; Longo, A.; Dam, B. Structure model for anion-disordered photochromic gadolinium oxyhydride thin films. *J. Phys. Chem. C* **2020**, *124*, 13541−13549.

(14) Anders, A. A structure zone diagram including plasma-based deposition and ion etching. *Thin Solid Films* **2010**, *518*, 4087−4090.

(15) Nafezarefi, F.; Cornelius, S.; Nijskens, J.; Schreuders, H.; Dam, B. Effect of the addition of zirconium on the photochromic properties of yttrium oxy-hydride. *Sol. Energy Mater. Sol. Cells* **2019**, *200*, 109923.

(16) Baba, E. M.; Montero, J.; Strugovshchikov, E.; Zayim, E. O.; Karazhanov, S. Light-induced breathing in photochromic yttrium oxyhydrides. *Phys. Rev. Mater.* **2020**, *4*, 025201.

(17) Montero, J.; Martinsen, F. A.; García-Tecedor, M.; Karazhanov, S. Z.; Maestre, D.; Hauback, B.; Marstein, E. S. Photochromic mechanism in oxygen-containing yttrium hydride thin films: An optical perspective. *Phys. Rev. B: Condens. Matter Mater. Phys.* **2017**, *95*, 201301.

(18) Montero, J.; Karazhanov, S. Z. Spectroscopic Ellipsometry and Microstructure Characterization of Photochromic Oxygen-Containing Yttrium Hydride Thin Films. *Phys. Status Solidi A* **2018**, *215*, 1701039.

(19) Maehlen, J. P.; Mongstad, T. T.; You, C. C.; Karazhanov, S. Lattice contraction in photochromic yttrium hydride. *J. Alloys Compd.* **2013**, *580*, S119−S121.

(20) Chandran, C. V.; Schreuders, H.; Dam, B.; Janssen, J. W. G.; Bart, J.; Kentgens, A. P. M.; van Bentum, P. J. M. Solid State NMR Studies of the Photochromic Effects of Thin Films of Oxygen Containing Yttrium Hydride. *J. Phys. Chem. C* **2014**, *118*, 22935.

(21) Plokker, M.; Eijt, S.; Naziris, F.; Schut, H.; Nafezarefi, F.; Schreuders, H.; Cornelius, S.; Dam, B. Electronic structure and vacancy formation in photochromic yttrium oxy-hydride thin films studied by positron annihilation. *Sol. Energy Mater. Sol. Cells* **2018**, *177*, 97−105.

(22) Eijt, S. W. H.; de Krom, T. W. H.; Chaykina, D.; Schut, H.; Colombi, G.; Cornelius, S.; Egger, W.; Dickmann, M.; Hugenschmidt, C.; Dam, B. Photochromic YOₓHᵧ Thin Films Examined by in situ Positron Annihilation Spectroscopy. *Acta Phys. Pol., A* **2020**, *137*, 205−208.

(23) Krause-Rehberg, R.; Leipner, H. S. *Positron Annihilation in Semiconductors: Defect Studies*; Springer Verlag: Berlin, 1999; p 93.

(24) Koto, K.; Schulz, H.; Huggins, R. A. Anion disorder and ionic motion in lead fluoride (β − PbF_2). *Solid State Ionics* **1980**, *1*, 355−365.

(25) Hagenmuller, P.; Réau, J.-M.; Lucat, C.; Matar, S.; Villeneuve, G. Ionic conductivity of fluorite-type fluorides. *Solid State Ionics* **1981**, *3−4*, 341−345.

(26) Bai, Q.; He, X.; Zhu, Y.; Mo, Y. First-principles study of oxyhydride H⁻ ion conductors: toward facile anion conduction in oxide-based materials. *ACS Appl. Energy Mater.* **2018**, *1*, 1626−1634.

(27) Liu, X.; Bjørheim, T. S.; Haugsrud, R. Formation of defects and their effects on hydride ion transport properties in a series of K_2NiF_4-type oxyhydrides. *J. Mater. Chem. A* **2018**, *6*, 1454−1461.

(28) Liu, X.; Bjørheim, T. S.; Vines, L.; Fjellvåg, Ø. S.; Granerød, C.; Prytz, Ø.; Yamamoto, T.; Kageyama, H.; Norby, T.; Haugsrud, R. Highly correlated hydride ion tracer diffusion in $SrTiO_{3-x}H_x$ oxyhydrides. *J. Am. Chem. Soc.* **2019**, *141*, 4653−4659.

(29) Yajima, T.; Takeiri, F.; Aidzu, K.; Akamatsu, H.; Fujita, K.; Yoshimune, W.; Ohkura, M.; Lei, S.; Gopalan, V.; Tanaka, K.; Brown, C. M.; Green, M. A.; Yamamoto, T.; Kobayashi, Y.; Kageyama, H. A labile hydride strategy for the synthesis of heavily nitridized BaTiO$_3$. *Nat. Chem.* **2015**, *7*, 1017−1023.

(30) Tang, Y.; Kobayashi, Y.; Shitara, K.; Konishi, A.; Kuwabara, A.; Nakashima, T.; Tassel, C.; Yamamoto, T.; Kageyama, H. On hydride diffusion in transition metal perovskite oxyhydrides investigated via deuterium exchange. *Chem. Mater.* **2017**, *29*, 8187−8194.

(31) Hans, M.; Tran, T. T.; Aoalsteinsson, S. M.; Moldarev, D.; Moro, M. V.; Wolff, M.; Primetzhofer, D. Photochromic mechanism and dual-phase formation in oxygen-containing rare-earth hydride thin films. *Adv. Opt. Mater.* **2020**, *8*, 2070078.

(32) Brennan, M. C.; Ruth, A.; Kamat, P. V.; Kuno, M. Photoinduced anion segregation in mixed halide perovskites. *Trends Chem.* **2020**, *2*, 282−301.